

Thickness of the pinned layer as a controlling factor in domain wall formation during training in IrMn-based spin valves

Jun Park,¹ Shannon M. Watson,² C. M. Furjanic,¹ D. K. Draganova,¹ S. D. Eisenberg,¹ D. J. Tighe,³ P. A. Kienzle,² M. J. Carey,⁴ J. A. Borchers,² P. D. Sparks,¹ and J. C. Eckert^{1,a)}

¹Physics Department, Harvey Mudd College, 301 Platt Blvd., Claremont, California 91711, USA

²NIST Center for Neutron Research, National Institute for Standards and Technology, 100 Bureau Drive, Stop 856-2, Bldg. 235, Gaithersburg, Maryland 20899, USA

³Department of Computer Science, Kent State University, P.O. Box 5190, Kent, Ohio 44242, USA

⁴Hitachi Global Storage Technologies, San Jose Research Center, 3403 Yerba Buena Road, San Jose, California 95135, USA

(Presented on 9 November 2007; received 14 September 2007; accepted 12 November 2007; published online 13 March 2008)

Studies of CoFe-based spin valves with antiferromagnetic IrMn layers as thin as 1.6 nm have demonstrated that a domain wall parallel to the surface develops in the pinned layer after training at the magnetoresistance (MR) maximum. To investigate the effects of domain wall formation on the MR, we have studied the depth profile of the vector magnetization in comparable spin valves, with pinned ferromagnetic (FM) layer thicknesses, from 1 to 15 nm, using polarized neutron reflectivity. At the maximum MR achieved after training, the antiparallel magnetization of the pinned layer, in a 2 nm sample, is reduced to 5% of its saturation value, suggesting the formation of domain walls perpendicular to the surface. In a 9 nm sample, the pinned layer magnetization is instead canted away from the field at the MR maximum. A transition from perpendicular to parallel domain wall formation occurs for pinned layer thicknesses greater than 4 nm, and the magnitude of the maximum MR subsequently depends on the type of domain wall that develops. © 2008 American Institute of Physics. [DOI: [10.1063/1.2837506](https://doi.org/10.1063/1.2837506)]

A spin valve (SV), whose applications range from hard drive read heads to magnetic biodetectors, is based on the exchange biasing effect. The essential components of a SV are an antiferromagnetic (AFM) layer that is exchange coupled to a pinned FM layer, a nonmagnetic spacer, and a free FM layer whose magnetic moment can align freely with the applied field. The strength of the exchange coupling in a spin valve can be measured indirectly through magnetoresistance (MR) measurements, yielding MR hysteresis loops such as those shown in Fig. 1. The exchange coupling of the pinned layer, however, has been reported to weaken after reversal of the magnetization of the pinned ferromagnetic (FM) layer which sets in when the applied magnetic field is sufficiently strong, resulting in a decreased exchange field H_{ex} and coercive field H_{co} ,¹⁻⁵ this result is known as the training effect. The training effect is also characterized by a reduced maximum MR ratio and a more gradual decrease in the MR as the field is increased, as shown in Fig. 1. Previous research⁶ on spin valves with a 1.6 nm AFM pinning layer has shown that the training effect in spin valves can be attributed to the formation of domain walls within the pinned layer that are parallel to the sample plane. However, the spatial extent of these parallel domain walls approximately matched the 3 nm width of the pinned FM layer. Spin valves with thinner pinned layers also exhibit training effects even though the formation of parallel domain walls in these FM layers may not be energetically feasible. For those SV's, the

shape of the MR loop is substantially different, and we thus expect that the type of domain wall formed may depend on the thickness of the pinned layer. To investigate the correlation between domain wall formation and MR training, we have studied a set of IrMn-based spin valves with a range of pinned layer thicknesses.

Our samples were grown using dc magnetron sputtering at Hitachi Global Storage Technologies in San Jose, CA. Layers were deposited onto $18 \times 18 \text{ mm}^2$ Si wafer with an oxidized layer, yielding the nominal structure Si/SiO₂/5.0 nm Ta/3.0 nm Ni₉₈Fe₂/1.0 nm Co₅₀Fe₅₀/3.0 nm Cu/ X nm Co₆₅Fe₃₅/1.6 nm Ir₂₀Mn₈₀/1.0 nm Cu/5.0 nm Ta with $X=1-15$ nm. Each sample was field cooled from room temperature in -0.65 T to pin the Co₆₅Fe₃₅ FM. In-plane giant magnetoresistance (GMR) measurements at 6 K yielded the MR hysteresis curves shown in Figs. 1(a) and 1(b) for the $X=2$ nm and $X=9$ nm samples, respectively. The behavior of the MR during the first cycle (black line) is typical of exchange-biased spin valves. The flat maximum presumably arises from an antiparallel alignment of the free and pinned FM layers, and the transition to the parallel state at high fields is sharp. The maximum MR ratio achieved during first field cycle peaks is plotted versus X in Fig. 1(c), and it exhibits a peak at $X=4$ nm. In addition, the exchange and coercive fields of different SV's are inversely proportional to the thickness of the pinned layer.^{7,8} During the second field cycle (red curve), we observe training in all samples, even in $X=1$ nm sample which has the largest H_{ex} of 0.39 T. This training is typified

^{a)}Electronic mail: eckert@hmc.edu.

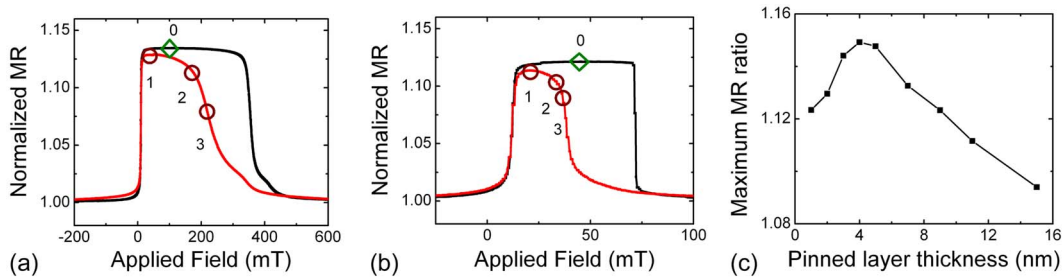


FIG. 1. (Color online) (a) Normalized MR vs field for $X=2$ nm spin valve at 6 K after cooling in $H=-0.65$ T. (b) Normalized MR vs field for $X=9$ nm sample at 6 K. The black curve is the first field cycle and the red curve is the second cycle. The circles and diamonds denote the fields at which the reflectivity measurements were performed. (c) Maximum MR ratio vs pinned layer thickness.

by a rounding of the MR maximum in all samples. However, the MR measurements reveal that the training effect observed in thin and thick samples are qualitatively different with a more gradual falloff of the MR in the former.

To investigate if this qualitative difference translates to a significant difference in the magnetic structures, we have measured polarized neutron reflectivity (PNR) for $X=2$ nm and $X=9$ nm samples at the NIST Center for Neutron Research (NCNR). For these PNR measurements, the incident and scattered neutrons with a wavelength of 0.475 nm were polarized parallel to the field cooling direction of the sample using Fe-Si supermirrors.⁹ Four different polarization cross sections were measured using Al-coil flippers before and after the sample. For the non-spin-flip (NSF) cross sections, R^{++} and R^{--} refer to neutrons that maintain their polarization, and for the spin-flip (SF) cross sections, R^{+-} and R^{-+} correspond to neutrons whose spin orientation is rotated 180° . The NSF data provide information about the chemical composition as a function of depth. In addition, the difference between R^{++} and R^{--} arises from the sample magnetization parallel to the polarization direction. The SF reflectivity is purely of magnetic origin and is nonzero only when there are macroscopic ($>100 \mu\text{m}$) magnetic domains within the sample plane with a magnetization component perpendicular to the polarization direction. All four reflectivity cross sections were corrected for the instrumental polarization efficiency (typically $>97\%$), instrumental background, and the footprint of the beam. To obtain the depth-dependent chemical structure and vector magnetization within the sample, the reduced data were fitted to the reflectivity formalism⁹ with the REFLPAK software,¹⁰ which is based on a least squares optimization. Additional fitting software, which utilizes the differential evolution algorithm,¹¹ was used to complement the REFLPAK software. The structural parameters, such as layer thicknesses, interface roughnesses, and others, obtained from the PNR fits were compared with those obtained from x-ray reflectivity fits to check for consistency.

After field cooling in -0.65 T, the PNR was measured at various fields along MR hysteresis loop, indicated by the diamonds and circles in Figs. 1(a) and 1(b), including the first MR maximum and saturation points. A typical data set is shown in Fig. 2(a) for $X=9$ nm sample, at 6 K, in a field of 0.0352 T, during the second field cycle. These data exhibit pronounced SF scattering, which is different from the PNR data obtained in saturating fields of 0.65 T or at the first MR maximum of 0.11 and 0.045 T for $X=2$ and 9 nm samples,

respectively. Those show negligible SF scattering, suggesting that there is no magnetization perpendicular to the applied field. Specifically, fits to the 0.11 T data for $X=2$ nm sample produce the depth profile for the magnetization depicted by the green line in Figs. 2(b) and 2(c). The magnetization of the pinned layer and free layer are antiparallel to each other, as expected, and the magnetization of the pinned layer is equal to that of the saturation state at $+0.66$ T. The magnetic structures of $X=2$ nm and $X=9$ nm samples undergo similar changes during the first field cycle. However, their magnetic structures deviate from each other significantly after the first field cycle.

Fits to PNR data for $X=2$ nm, at 0.0356 T, during the second cycle [circle 1 in Fig. 1(a)], suggest that the magnetic structure is very similar to that obtained in a field of $+0.11$ T during the first field cycle. As the field was increased to $+0.19$ T [circle 2 in Fig. 1(a)], however, the magnetization of the pinned $\text{Co}_{65}\text{Fe}_{35}$ layer is almost halved [purple fill in Fig. 2(b)] though the magnetization in the free FM layer remains intact. As the field was further increased to 0.23 T [circle 3 in Fig. 1(a)], the net magnetization of the pinned layer is reduced to 5% of its saturation value [purple fill in Fig. 2(c)]. PNR data show negligible SF scattering at all these fields

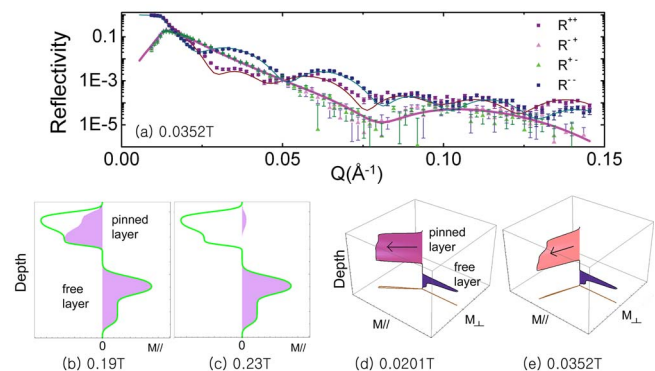


FIG. 2. (Color online) (a) Polarized neutron reflectivity of 9 nm sample measured at 6 K in 0.0352 T during the second field cycle. R^{++} and R^{--} correspond to the NSF cross sections and R^{+-} and R^{-+} correspond to the SF cross sections. The lines correspond to fits to the data. The green lines in (b) and (c) are the magnetic depth profile for the sample with 2 nm pinned layer during the first field cycle at $+0.11$ T [green diamond in Fig. 1(a)]. The purple fill in (b) and (c) is the depth profile during the second field cycle at $+0.19$ and $+0.23$ T, respectively [brown circles in Fig. 1(b)]. Figures (d) and (e) are the depth profiles of magnetization in $X=9$ nm sample at $+0.0201$ and $+0.0352$ T.

indicating that the moment in the pinned layer is not canted and a magnetic spiral is not present. Instead, it is likely that magnetic domains (smaller than $10\ \mu\text{m}$) form across the sample plane, and the magnetization averaged across the sample plane is then reduced from the saturation value. Our fits to the PNR data for $X=2\ \text{nm}$ [Figs. 2(b) and 2(c)], thus support the formation of in-plane domains with domain walls perpendicular to the sample plane during training, and this reduction in the moment gives rise to the gradual reduction of the MR with increasing field.

In $X=9\ \text{nm}$ sample, the magnetic structure at the MR maximum in the second cycle differs significantly from the antiparallel state observed during the first field cycle. PNR data measured at a field of $0.0201\ \text{T}$ [point 1 in Fig. 1(b)] exhibit strong SF scattering, suggesting that there is a component of the magnetization perpendicular to the field. Fits to the PNR indicate that the moment in the pinned layer is not reduced from its saturation value, but, instead, is canted away from the field direction by 33° , as shown in Fig. 2(c). As the field is increased to $0.0343\ \text{T}$, the magnetization in the pinned layer, near the AFM-FM interface, is reduced slightly and the cant angle increases to 58° . As we further increase the field to $0.0352\ \text{T}$, the magnetization of the CoFe layer is further decreased to 90% of its saturation value and the cant angle increases to 67° , as shown in Fig. 2(d). Fits to PNR data in all three cases, indicate that the angular spread of the canted moment within the pinned FM layer is less than 10° . The gradual reduction of the MR with increasing field seen in Fig. 1(b) in this case originates primarily from a canting of the pinned layer moment relative to the field direction. This coherent rotation of the magnetization has a similar character to the spiral domain walls parallel to the sample surface that were reported for a similar spin valve with a $3\ \text{nm}$ pinned layer.⁶

Through GMR measurements we have determined that SV's with pinned FM layer thicknesses, ranging from 1 to 15 nm, exhibit MR maxima that depend on the layer thickness. These same spin valves also show pronounced training effects. The gradual reduction of the MR with increasing field is correlated with the formation of in-plane domains and perpendicular domain walls in spin valves with a relatively thin pinned layer, whereas those with a thicker pinned layer develop parallel domain walls and/or a canting of the magnetization. We speculate that the energetics prohibit the formation of parallel domain walls in the thin layers and there thus exists a critical thickness below which parallel domain walls are no longer favored. For our sample set, this critical transition lies between 2 and 9 nm and may give rise to the peak GMR ratio which occurs in $X=4\ \text{nm}$ sample. Further PNR measurements of spin valves with intermediate thickness will give us more information about this transition.

This work was supported in part by the NSF through Grant No. 0421565.

- ¹D. Paccard, C. Schlenker, O. Massenet, R. Montmory, and A. Yelon, *Phys. Status Solidi* **16**, 301 (1966).
- ²M. D. Stiles and R. D. McMichael, *Phys. Rev. B* **60**, 12950 (1999).
- ³S. J. Yuan, L. Wang, S. M. Zhou, M. Lu, J. Du, and A. Hu, *Appl. Phys. Lett.* **81**, 3428 (2002).
- ⁴M. Ali, C. H. Marros, and B. J. Hickey, *Phys. Rev. B* **67**, 172405 (2003).
- ⁵T. Hauet, J. A. Borchers, Ph. Mangin, Y. Henry, and S. Mangin, *Phys. Rev. Lett.* **96**, 067207 (2006).
- ⁶S. Moyerman, J. C. Eckert, J. A. Borchers, K. L. Perdue, M. Doucet, P. D. Sparks, and M. J. Carey, *J. Appl. Phys.* **99**, 08R505 (2006).
- ⁷J. Nogués and I. K. Schuller, *J. Magn. Magn. Mater.* **192**, 203 (1999).
- ⁸D. Mauri, E. Kay, D. Scholl, and J. Kent Howard, *J. Appl. Phys.* **62**, 2929 (1987).
- ⁹C. F. Majkrzak, *Physica B* **221**, 342 (1996).
- ¹⁰P. K. Kienzle (http://www.ncnr.nist.gov/programs/reflect/data_reduction/software/index.html).
- ¹¹D. Tighe and P. K. Kienzle (private communication).